



A Wide Range of Testing Results on an Excellent Lithium-Ion Cell Chemistry to be used as Benchmarks for New Battery Technologies

Jessie E. Harlow,^{1,2} Xiaowei Ma,^{1,2} Jing Li,^{1,2} Eric Logan,^{1,2} Yulong Liu,^{1,2} Ning Zhang,^{1,2} Lin Ma,^{1,2} Stephen L. Glazier,^{1,2} Marc M. E. Cormier,^{1,2} Matthew Genovese,^{1,2,*} Samuel Buteau,^{1,2} Andrew Cameron,^{1,2} Jamie E. Stark,^{1,2} and J. R. Dahn^{1,2,**,z}

¹Department of Physics and Atmospheric Science, Dalhousie University, Halifax, N.S B3H 4R2, Canada

²Department of Chemistry, Dalhousie University, Halifax, N.S B3H 4R2, Canada

We present a wide range of testing results on an excellent moderate-energy-density lithium-ion pouch cell chemistry to serve as benchmarks for academics and companies developing advanced lithium-ion and other “beyond lithium-ion” cell chemistries to (hopefully) exceed. These results are far superior to those that have been used by researchers modelling cell failure mechanisms and as such, these results are more representative of modern Li-ion cells and should be adopted by modellers. Up to three years of testing has been completed for some of the tests. Tests include long-term charge-discharge cycling at 20, 40 and 55°C, long-term storage at 20, 40 and 55°C, and high precision coulometry at 40°C. Several different electrolytes are considered in this LiNi_{0.5}Mn_{0.3}Co_{0.2}O₂/graphite chemistry, including those that can promote fast charging. The reasons for cell performance degradation and impedance growth are examined using several methods. We conclude that cells of this type should be able to power an electric vehicle for over 1.6 million kilometers (1 million miles) and last at least two decades in grid energy storage. The authors acknowledge that other cell format-dependent loss, if any, (e.g. cylindrical vs. pouch) may not be captured in these experiments.

© The Author(s) 2019. Published by ECS. This is an open access article distributed under the terms of the Creative Commons Attribution 4.0 License (CC BY, <http://creativecommons.org/licenses/by/4.0/>), which permits unrestricted reuse of the work in any medium, provided the original work is properly cited. [DOI: 10.1149/2.0981913jes]



Manuscript submitted July 30, 2019; revised manuscript received August 16, 2019. Published September 6, 2019.

Lithium-ion cells are being used in grid energy storage and in electric vehicles where long lifetime is extremely important. At this time, many of these applications are generally not as demanding as they might seem. This is because it can be rare that cells are subjected to 100% depth of discharge cycling again and again on a daily or several times daily basis. For example, Pearre et al.¹ show that the average daily driving range for 484 gasoline vehicles in the US was 32.6 miles (52 km) and that the vast majority of daily range need is in the 0–50 mile range (0 – 80 km). For an EV with a 300 or 400 km range this represents about 25% DOD on a daily basis. Many researchers have shown that the lifetime of lithium-ion cells measured in cumulative charge throughput is much longer when low DOD duty cycles are applied (e.g.)^{2,3}

This situation may change with the proposed introduction of “robo taxis”, long haul electric trucks and vehicle-to-grid applications. In the former, vehicles will be driving all day, much like a conventional taxi and undergoing nearly 100% DOD cycling. Long haul trucks will almost certainly run in near 100% DOD situations. Cells in vehicles tethered to the grid will be racking up charge-discharge cycles even when the vehicle is not moving. Clearly EVs destined for vehicle-to-grid applications, robo taxis or long haul trucking, would favor a lithium-ion chemistry that could deliver many more charge-discharge cycles in a decade than an EV that was destined for typical commuter driving where high energy density to give the longest driving range for weekend trips might be emphasized. Electric buses represent another application where duty cycles approaching 100% DOD are used on a daily basis.⁴

In order to make reasonable projections about lifetime, it is insufficient to simply do charge-discharge cycle testing at high rate (for example 1C). For example, if a particular cell type can provide 1000 100% DOD charge-discharge cycles at 1C, this could be claimed to be able to power a 400 km range EV for 400,000 km. In such a testing scenario, 10–12 cycles per day can be collected and the entire test would only take about 100 days. Instead careful considerations of aging during cycling and aging during storage must be made as has been done by many researchers. For example, in 2019 Jana et al.⁵ show how “the identification of the individual degradation contributions enables the possibility of tailoring the charge/discharge sequence

to extend battery life.” Jana et al. compare their models to data presented in the literature on NMC/graphite Li-ion cells by Ecker et al.,² Schmitt et al.,⁶ Schuster et al.,⁷ among others and show excellent agreement. In 2018, Dubarry et al.,⁸ reviewed calendar aging studies on a variety of Li-ion cell chemistries, including NMC/graphite and LiFePO₄(LFP)/graphite, among others. Dubarry et al., use data from references^{2,6,7} and⁹ for NMC/graphite cells, data from Naumann et al.,¹⁰ among others, for LFP cells, and data from Keil et al.,¹¹ among others, for NCA cells.

The cycle and calendar lifetime of NMC/graphite cells has improved dramatically since the time references^{2,5,6,8} were published. In addition, many researchers, OEMs and battery users believe the cycle and calendar lifetime of LFP/graphite cells are superior to that of NMC/graphite cells. We believe it is important to disseminate state-of-the-art data for NMC/graphite cells to aid future modelling efforts and to provide modern benchmarks for both old and new cell technologies.

In this paper, testing results on LiNi_{0.5}Mn_{0.3}Co_{0.2}O₂/artificial graphite (NMC532/AG) cells are presented. The NMC532 used in these cells is “single crystal” NMC532 as described in the papers by Jing Li et al.¹² and Lin Ma et al.^{13–15} The artificial graphite (AG) used in these cells is provided by Kaijin (China) and is grade AML-400. Over the last 10 years the Dalhousie research group has tested a wide variety of Li-ion cells with various positive electrodes, negative electrodes and electrolytes.^{12–19} Of all the cells tested, the ones with the longest lifetime are the single crystal NMC532/AG cells with optimized electrolytes reported here. Therefore, we believe it is valuable to present a comprehensive summary of this test data for others to benchmark against.

The data in this paper focuses on long-term tests at 20, 40 and 55°C. These temperatures were selected based on historical precedents in our group. We do note that many Li-ion cell manufacturers and other researchers present data at 25, 30, 45, 50, 55 and 60°C, some of which are offset from our data. In the long-term cycle testing, preference is given to studies over 100% DOD which is between 3.0 and 4.3 V for the cells considered here. However, some testing results are given for lower DOD ranges such as 3.0 to 4.2 V and 3.0 to 4.1 V to show the advantages that charging to a lower voltage can bring in both cycling and storage.

To capture the attention of the reader, Figure 1 compares long-term charge-discharge cycle performance of the cylindrical NMC/graphite cells (Sanyo UR18650E) tested by Ecker et al.² to some of the pouch cells in this work. Details of the cells used in this work will be given later, as will a full set of performance data. The 100% DOD cycling

*Electrochemical Society Student Member.

**Electrochemical Society Fellow.

^zE-mail: jeff.dahn@dal.ca

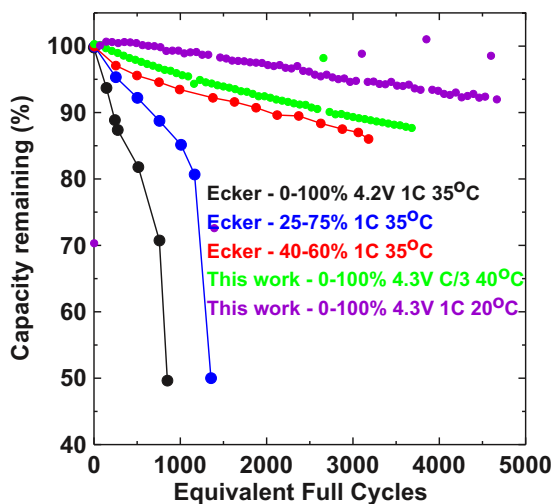


Figure 1. Long-term cycling data plotted as percent initial capacity versus equivalent full cycles for NMC/graphite cells as described in the legend. The data from this work for 100% DOD cycling was collected to an upper cutoff potential of 4.3 V. The data from Ecker et al.,² used 4.2 V as 100% state of charge. The purple and green data (this work) should be compared to the black data (Ecker et al.). Data for restricted range cycling (i.e. 25 - 75% SOC and 40 - 60% SOC) for the cells in this work is not available but is expected to be far better than the data shown for 0 - 100% DOD cycling by analogy with the cells tested by Ecker et al.

of the cells in the present work is far superior to that of the Sanyo cells even though the upper cutoff potential was 4.3 V compared to 4.2 V.

Figure 2 shows long-term storage data of NMC/graphite cells studied by Ecker et al.² and Schmitt et al.⁶ to the cells of this work. The cells studied by Schmitt et al.⁶ were cylindrical model US18650V3 from Sony Energy Devices Corporation. Reference performance test-

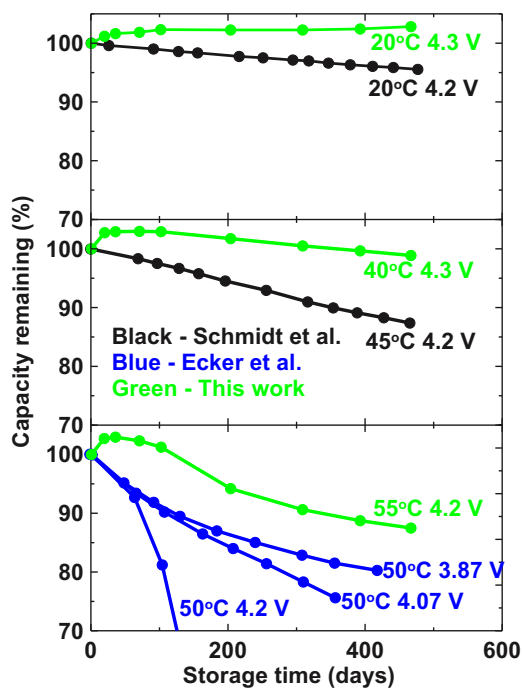


Figure 2. Capacity remaining versus storage time for NMC/graphite cells as determined by reference performance testing every several months. The data from Ecker et al.² and Schmitt et al.⁶ are for Sanyo UR18650E and Sony US18650V3 cells, respectively. The voltages and temperatures at which the cells were stored are given in the legends.

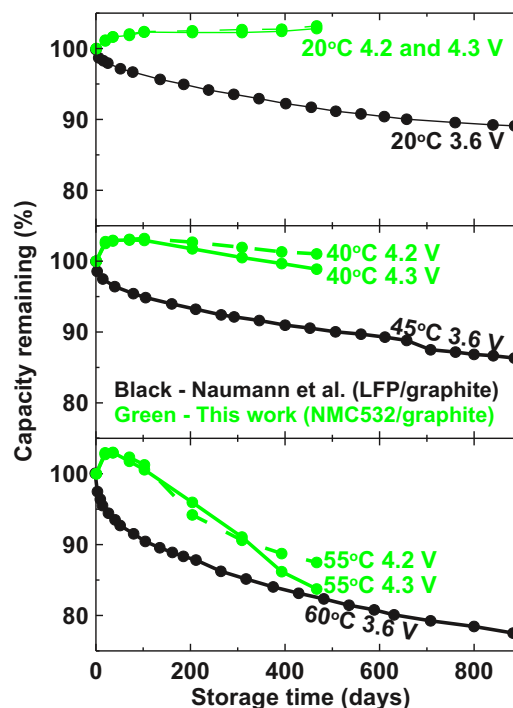


Figure 3. Percent capacity remaining versus storage time for LFP/graphite cells (Sony US26650FTC1) from Naumann et al.¹⁰ and for the cells in this work as determined by periodic reference performance testing (RPT). The voltages and temperatures at which the cells were stored are given in the legends.

ing (RPT) was performed periodically to determine the remaining cell capacity as a function of storage time. Figure 2 shows that the pouch cells in this work far outperform the cylindrical cells tested by Ecker et al. and Schmitt et al. Researchers and users of Li-ion cells should be aware of this vast performance increase that is possible.

Figure 3 shows long-term storage results for the NMC/graphite cells of this work compared to results for cylindrical LFP/graphite cells from Naumann et al.¹⁰ The cells tested by Naumann et al. were US26650FTC1 cells from Sony. Figure 3 shows that the long-term storage results for the NMC/graphite pouch cells of the present work are at least as good as the results for these LFP/graphite cells even though the storage voltages at 100% (4.3 V) and 90% SOC (4.2 V) for the NMC cells are much higher than that of the LFP cells (3.6 V) at 100% SOC. Researchers and users of Li-ion cells should be aware that NMC/graphite cells of an appropriate design, to be described in this paper, can have longer storage lifetimes than LFP/graphite cells. Since NMC/graphite cells have much larger volumetric and specific energy densities than LFP/graphite cells²⁰ one does not need to make a trade-off between energy density and lifetime anymore.

It is the intention of Figures 1, 2 and 3 to have whetted the appetite of the reader to learn more about the cells of this work to be described below.

Experimental

Pouch cells.—Dry (no electrolyte) and sealed $\text{Li}[\text{Ni}_{0.5}\text{Mn}_{0.3}\text{Co}_{0.2}]\text{O}_2$ (NMC532)/graphite pouch cells were obtained from Li-FUN Technology (Xinma Industry Zone, Golden Dragon Road, Tianyuan District, Zhuzhou City, Hunan Province, China, 412000). These were coated NMC532/artificial graphite (240 mAh at 4.3 V). The NMC532 used in these cells was single crystal NMC532 as described by Li et al.¹² with a Ti-based coating as described by Ma et al.¹⁴ The artificial graphite used was Kaijin AML-400 from Kaijin, China. The single side active material electrode loadings were 21.1 mg/cm² for the positive electrode and 12.2 mg/cm² for the graphite negative electrode. The positive

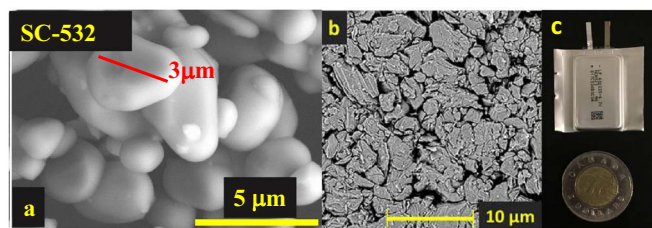


Figure 4. a) SEM image of the single crystal NMC532 powder (SC-532); b) Top view SEM image of the AML-400 negative electrode surface after compression; c) shows an image of one of the 402035-size pouch cells next to a Canadian \$2 coin (a “toonie”).

and negative electrodes consisted of 94 wt.% and 95.4 wt.% active materials, respectively. The positive electrode was compressed to 3.5 g/cm³ and negative electrode was compressed to 1.55 g/cm³. Prior to filling with the designed electrolytes, pouch cells were cut open and dried at 100°C under vacuum for 14 h to remove residual moisture. Afterwards, pouch cells were filled with 0.85 mL electrolyte in an Ar-filled glove box and sealed with a pouch sealer (MSK-115A Vacuum Sealing Machine) under vacuum at a pressure of -90 kPa (relative to atmospheric pressure). Figure 4a shows an SEM image of the single crystal NMC532 powder while Figure 4b shows a top view SEM image of the negative electrode surface. Figure 4c shows an image of one of the 402035-size pouch cells next to a Canadian \$2 coin (a “toonie”).

The cells in this work have a designed capacity of about 240 mAh at C/20. Table 1a shows the actual specific energy and energy density of the pouch cells used in this work. Even though these are very small cells where the area of the pouch is much larger than the area of the jelly roll, the specific energy is still 200 Wh/kg. The energy density is relatively low compared to that of a larger cell. To give readers some idea of the energy density that could be obtained in a larger cell, Table 1b shows the “stack energy density” for three designs which mirror what was used in the 402035 cells but with differing electrode thicknesses. The stack energy density accounts for everything except the additional volume due to the cell casing, dead space and excess electrolyte. Typically real energy densities can be 75% of the stack energy density for cells of a few Ah capacity. For example a 21700-size NMC532/graphite cell from a reputable manufacturer has a mass

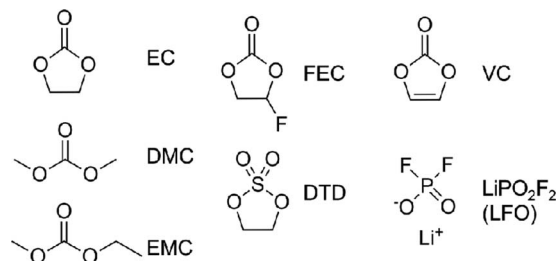


Figure 5. Solvents and additives used in the electrolytes incorporated into the pouch cells used in this work. EC = ethylene carbonate (CAS# = 96-49-1), DMC = dimethyl carbonate (CAS# = 616-38-6), EMC = ethyl methyl carbonate (CAS# = 623-53-0), FEC = fluoroethylene carbonate (CAS# = 114435-02-8), DTD = ethylene sulfone (CAS# = 1072-53-3), VC = vinylene carbonate (CAS# = CAS No.872-36-6), LiPO₂F₂ (called LFO here) = lithium difluorophosphate (CAS# = 24389-25-1).

of 62.5 g, a volume of 24.3 cm³ and a capacity of 3.75 Ahr when charged to 4.3 V (which is the design upper cutoff voltage for the 402035 pouch cells used here). Assuming an average voltage of 3.75 V, this corresponds to a specific energy of 225 Wh/kg and an energy density of 580 Wh/L. The energy density of this 21700 cell is 72.5% of the stack energy of the cell design used in this paper (see Table 1b).

All of the cells in this work were bar coded so that their results could be included in laboratory data bases. Although unconventional, we have included the barcodes for the cells in many of the legends of the graphs of results. This is because many of the cells discussed here are still running ongoing tests. Interested readers can contact the authors to obtain updates on one or more cells by referring to barcode numbers.

Electrolytes used.—There were several electrolytes used over the course of this work. The chemicals used in the electrolytes are shown in Figure 5. All these chemicals, plus methyl acetate (MA) and LiPF₆ (not shown in Figure 5), were battery grade, obtained from Shenzhen Capchem (China) and used as received.

The electrolyte solvent blends used in this work were EC:EMC 3:7 (by weight), EC:DMC 3:7 (by weight), EC:EMC:DMC 25:5:75 (by volume) and EC:EMC:MA 3:5:2 (by weight). All electrolytes used either 1.0, 1.2, 1.5 or 1.8 M LiPF₆ salt sourced from either BASF or

Table 1. a) Measured properties of the NMC532/graphite 402035 (40 mm x 20 mm x 3.5 mm thick) pouch cells used here. The positive electrode was 94% active material, the loading was 21.1 mg/cm² (target was 21.3) and the electrode density was 3.5 g/cm³. The negative electrode was 95.4% active material, the loading was 12.2 mg/cm² (target was 11.8) and the electrode density was 1.55 g/cm³. b) Stack energy density of the NMC532/graphite couple for several electrode thicknesses. b) Stack energy density calculations – gives values for the electrode stack (negative coating/copper/negative coating/separator/positive coating/aluminum/positive coating/separator). Assumptions – copper foil = 8 μm, aluminum foil = 15 μm, separator = 16 μm, N/P capacity ratio = 1.1 at 4.3 V, average cell voltage = 3.75 V. The highlighted row represents the design used in this work.

a)										
Cell designation	Average Voltage	Capacity (mAh)	Mass (g)	Volume (cm ³)	Specific Energy (Wh/kg)	Energy Density (Wh/L)	Positive areal capacity (mAh/cm ²)			
403025	3.75	240	4.5	2.3	200	390	3.5			
b)										
Cathode loading (mg/cm ²)	Cathode active material fraction	Cathode density (g/cm ³)	Cathode reversible capacity (mAh/g)*	Cathode irreversible capacity (%)	Anode loading (mg/cm ²)	Anode active material fraction	Anode density (g/cm ³)	Anode reversible capacity (mAh/g)	Anode irreversible capacity (%)	Stack Energy Density (Wh/L)
21.3	94	3.5	175	10	11.8	95.4	1.55	350	8	795
25.0	94	3.5	175	10	13.85	95.4	1.55	350	8	815
30.0	94	3.5	175	10	16.6	95.4	1.55	350	8	836

*measured at 30°C and C/10 between 3.0 and 4.3 V.

Shenzhen Capchem. We have seen no penalty associated with lifetime reduction using the first three solvent blends, unless high rate charge ($> 1C$ at $20^{\circ}C$) is attempted. The DMC containing blends are preferred due to higher ionic conductivity for high rate charge.²¹ If even higher rates of charge are desired, then methyl acetate can be added as in the fourth solvent blend. Figure 6 shows the conductivity of several electrolyte systems as a function of $LiPF_6$ content at $20^{\circ}C$ and also their temperature dependence at 1 molal. Figure 6 shows the advantage of EC:DMC over EC:EMC and the advantage of adding MA. Electrolytes with DMC are preferred over those with EMC when high rate charge or discharge is desired. Additions of MA cause a lifetime reduction for NMC/graphite cells²² so one must realize that a trade-off between lifetime and higher rate capability is being made when MA is introduced. This trade-off is explored in this article.

The cells in this study used several electrolyte additives which have been shown previously to dramatically increase lifetimes. The combination of 2% VC + 1% DTD promoted by Li et al.,¹² the combination of 2% FEC + 1% LFO promoted by Ma et al.¹⁶ and 1% LFO alone promoted by Ma et al.,¹³ were used in the cells in this work.

Testing protocols used.—Long-term storage was performed by placing cells at various voltages in convection ovens at 20, 40 or $55^{\circ}C$ for extended periods of time. Periodically, cells were extracted and subjected to a reference performance test (RPT) as shown in the left panel of Figure 7. The C/3 capacity, measured between 3.0 and 4.1 V at $20^{\circ}C$ was monitored. After the RPT test, the cells were charged to the original storage voltage at C/3 CCCV (C/100 current limit) and placed back in their respective ovens.

Long-term cycle testing was performed using battery testers from Neware (Shenzhen, China). Cycling was normally between 3.0 and 4.3 V using a C/3 rate at 20, 40 and $55^{\circ}C$. Charging used CCCV mode with a C/20 current cutoff. Some testing was made at $20^{\circ}C$ using 1C charge and discharge with CCCV charge to a C/20 current limit. The 1C testing also included a “rate map” with discharge currents of C/20, C/2, C, 2C and 3C where the charging currents were C/20 for the C/20 discharge cycle and 1C (with a CCCV to C/20) for all the other cycles in the rate map. The rate map protocol is shown in the center panel of Figure 7.

The difference between the average charge voltage and the average discharge voltage, ΔV , was measured and used as a measure of cell internal resistance. ΔV was calculated as shown in the right panel of Figure 7. Graphs of ΔV versus cycle number or time are used to monitor the stability of cell internal resistance. This can also be gleaned

from the variation of the 3C cell capacity versus cycle number in the rate maps.

Cross-Sectional scanning electron microscopy of cycled positive electrodes.—Cross sectional SEM images were taken of positive electrodes from cycled pouch cells. Cells after long duration testing were charged to 4.3 V and opened carefully in an argon-filled glove box. Circular discs of 1.1 cm diameter were punched from the positive electrode. Electrodes were rinsed with dimethyl carbonate twice before ion-milling with IB-19530CP cross-section polisher. Electrodes were milled with an Ar-ion beam for a 50 minute and 6 kV coarse step followed by a 5 minute and 6 kV fine step. SEM images were taken using a Hitachi S-4700 field emission electron microscope with a secondary electron detector. The images were obtained using an accelerating voltage of 5 kV and current of 15 μA .

Results and Discussion

Charge-discharge cycling results.—Figures 8 and 9 provide capacity retention versus cycle number data and normalized ΔV versus cycle number data for the NMC532/graphite cells testing between 3.0 and 4.3 V (0 – 100% SOC, Figure 8) and between 3.0 and 4.2 V (0 – 90% SOC, Figure 9). The cells tested at C/3 used 1.0 M $LiPF_6$ in EC:EMC 30:70 electrolyte with the selected additives indicated in the Figure legend while the cells tested at 1C used 1.2 M (2FEC + 1LFO) or 1.5 M (2VC+1DTD) $LiPF_6$ in EC:EMC:DMC 25:5:70 electrolyte. The duration of the testing is indicated in the legend. The appropriate data in Figure 8 was used in the comparison provided to Ecker et al.’s.² data as Figure 1. The reader should note the extremely expanded vertical scales in Figures 8 and 9, which vary from panel to panel.

Figure 8 shows that the additive blend 2% FEC + 1% LFO provides a substantial advantage at $20^{\circ}C$ compared to 2%VC + 1% DTD. However, at elevated temperature, the situation is reversed. So the choice of additives could be application specific. In any case, the data in Figure 8 is far better than any literature data we have seen for NMC/graphite cells tested between 0 and 100% SOC. Comparing Figures 8 and 9 reveals that the main benefit of lowering the upper cutoff potential is better control of impedance growth at 20 and $40^{\circ}C$.

Figure 10 shows capacity versus cycle number for NMC532/graphite cells tested at 1C with rate maps and at $20^{\circ}C$. Figures 10a and 10b show that the cycling of these cells is incredibly impressive between 3.0 and 4.1 V with no measurable loss in 3C capacity. Figure 10c shows that when the additive mixture

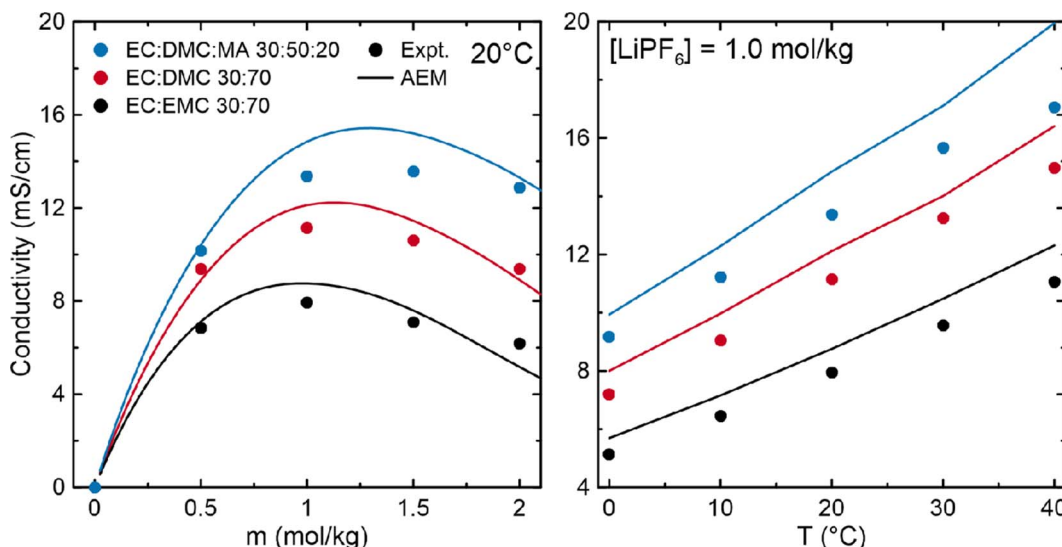


Figure 6. a) Conductivity at $20^{\circ}C$ versus molality in $LiPF_6$ EC:DMC:MA 30:50:20, EC:DMC and EC:EMC electrolytes. b) Conductivity versus temperature for 1.0 M $LiPF_6$ in the same solvent blends. The solid lines are the predictions of Gering's Advanced Electrolyte Model (AEM).²³

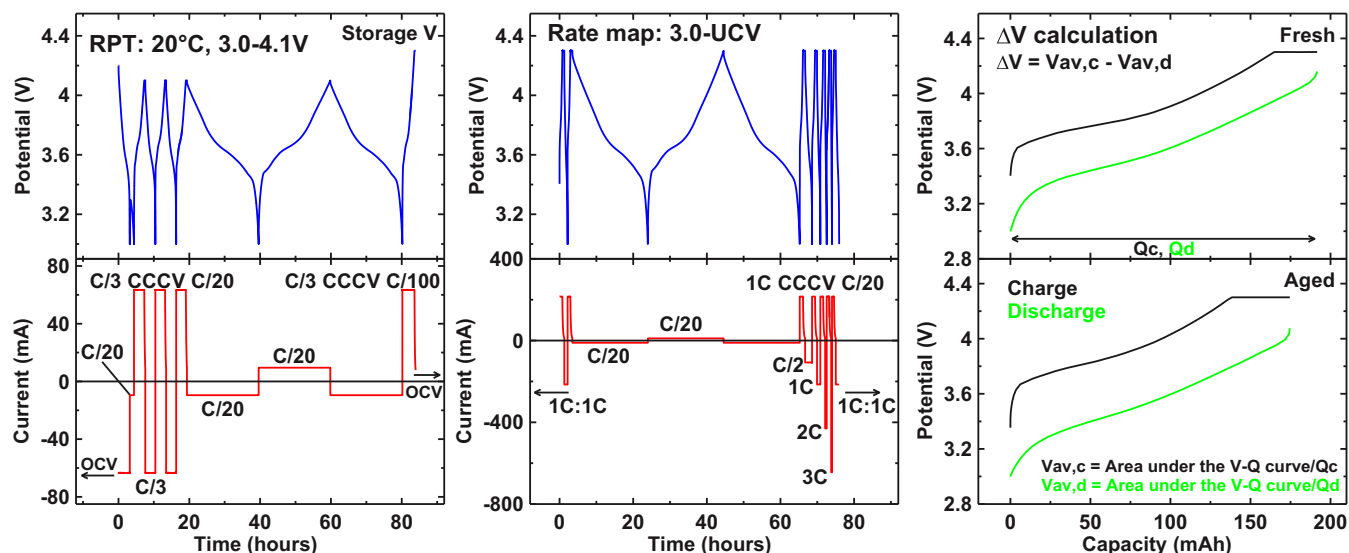


Figure 7. Left panel) Showing the reference performance test protocol used to periodically monitor the cells under storage testing; center panel) Protocol used in the rate maps collected every 100 cycles of cells cycled at 1C at 20°C; right panel) Schematically indicating how ΔV is calculated.

2%VC + 1%DTD is used there is a loss in 3C capacity during testing between 3.0 and 4.3 V. Figure 10d shows that when the additive mixture 2% FEC + 1% LFO is used there is virtually no 3C capacity loss even after 5400 cycles between 3.0 and 4.3 V. Figures 10e and 10f show that the 3C capacity is even better maintained when higher LiPF₆ concentrations are used for cells with 2% FEC + 1% LFO tested between 3.0 and 4.3 V.

Readers may wonder why the C/20 capacity versus cycle number in Figure 10 slowly decays with cycle number while the 1C capacity decays more slowly. This is explained in the text surrounding Figures 6 in Reference 16.

Figure 11 shows the voltage - capacity curves of the discharge of the cells described by Figure 10 measured during the rate maps. The 8 curves of each color were taken at equally spaced intervals

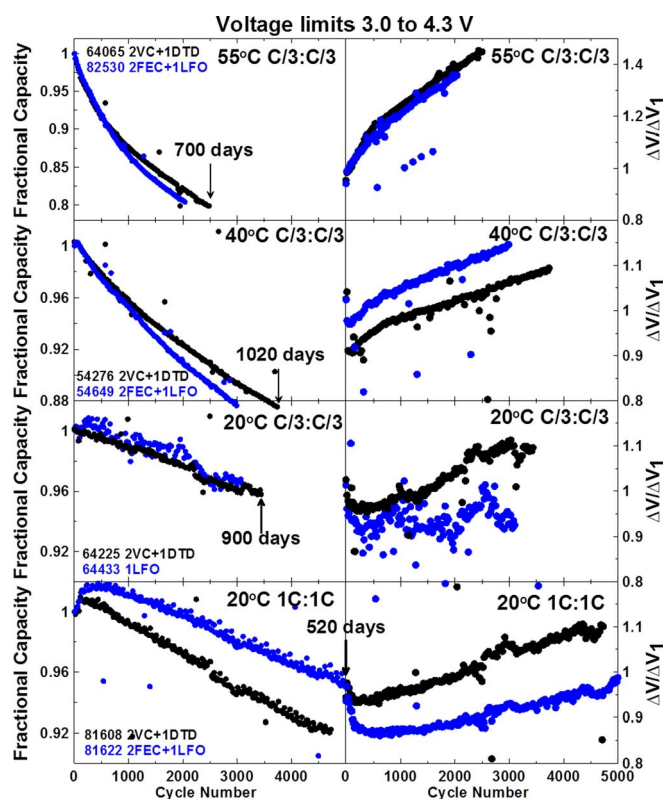


Figure 8. Fractional capacity and normalized ΔV plotted versus cycle number for NMC532/graphite cells tested between 3.0 and 4.3 V under the conditions shown in the legends. The duration of testing is shown for the most mature cells.

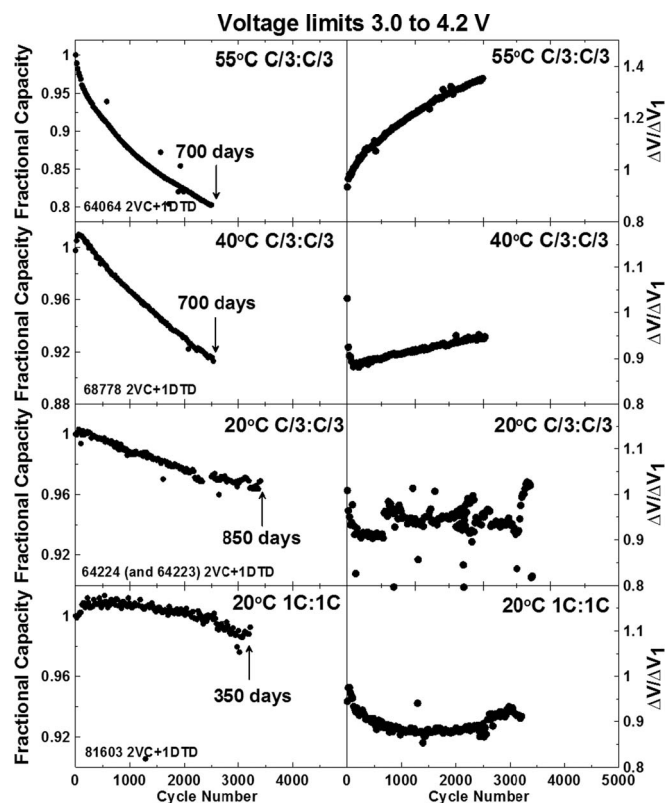


Figure 9. Fractional capacity and normalized ΔV plotted versus cycle number for NMC532/graphite cells tested between 3.0 and 4.2 V under the conditions shown in the legends. The duration of testing is shown for the most mature cells.

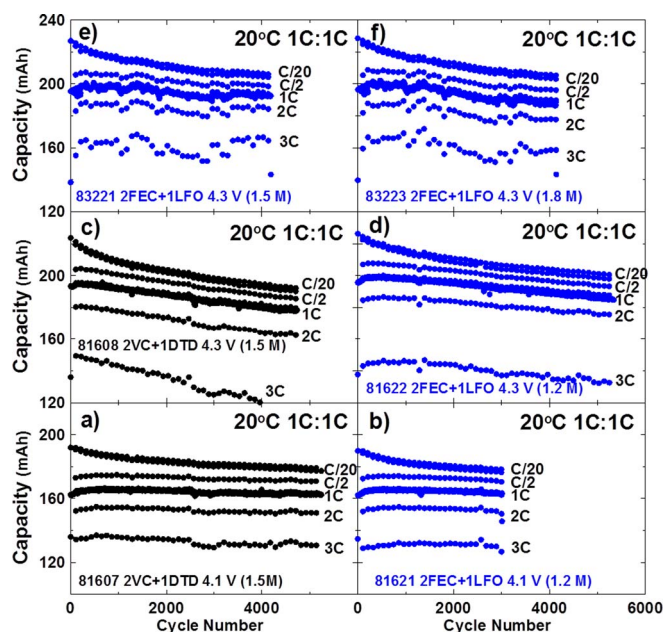


Figure 10. Results of 1C testing of NMC532/graphite cells at 20°C with rate maps every 100 cycles. The C/20, C/2, 1C, 2C and 3C markers show the discharge capacity of the corresponding discharge at the indicated rate. a) 1.5 M LiPF₆ in EC:EMC:DMC 25:5:70 with 2% VC + 1% DTD tested between 3.0 and 4.1 V; b) 1.2 M LiPF₆ in EC:EMC:DMC 25:5:70 with 2% FEC + 1% LFO tested between 3.0 and 4.1 V; c) 1.5 M LiPF₆ in EC:EMC:DMC 25:5:70 with 2% VC + 1% DTD tested between 3.0 and 4.3 V; d) 1.2 M LiPF₆ in EC:EMC:DMC 25:5:70 with 2% FEC + 1% LFO tested between 3.0 and 4.3 V; e) 1.5 M LiPF₆ in EC:EMC:DMC 25:5:70 with 2% FEC + 1% LFO tested between 3.0 and 4.3 V; f) 1.8 M LiPF₆ in EC:EMC:DMC 25:5:70 with 2% FEC + 1% LFO tested between 3.0 and 4.3 V. Data for cells that use the 2% VC + 1% DTD additive blend are shown in black while data for cells that use the 2% FEC + 1% LFO additive blend are shown in blue.

along the capacity versus cycle number curves. Figures 11a and 11b show that there is virtually no impedance growth in the cells cycled to 4.1 V as can be determined from the virtual overlap of the 3C discharge curves for 5200 (Figure 11a) and 3100 (Figure 11b) cycles. By contrast, Figures 11c and 11d do show evidence of impedance increase when cells are charged to 4.3 V because the 3C discharge curves shift down sequentially during the cycle testing. Figures 11e and 11f show that increasing the LiPF₆ concentration in the presence of the 2% FEC + 1% LFO additive virtually eliminates impedance growth during cycling to 4.3 V at 3C even over 4100 cycles.

Figure 11 also can be used to determine that major cause of C/20 capacity loss in these cells is lithium inventory loss. Careful examination of the eight C/20 discharge curves in each of Figures 11a–11f shows that the portion of the curves above 3.6 V are unchanged over the duration of the cycles. This indicates no active material loss. The loss of capacity occurs only in the lower voltage region. This is caused by a shift of the negative electrode voltage-capacity curve relative to the positive electrode voltage-capacity curve due to lithium inventory loss. It will be shown later, using differential voltage (dV/dQ vs. Q) analysis that the only capacity loss mechanisms in these cells are lithium inventory loss and impedance growth, in cases where the latter occurs.

We wondered if the increase of ΔV with cycle number at 40°C and 55°C shown in Figures 8 and 9 would affect subsequent operation at 20°C. Figure 12 shows the capacity versus cycle number for NMC532/graphite cells that operated for about 1 year at 40°C or 55°C and were then moved to 20°C for continued testing for another year or so. Figures 12a and 12b show that when the cell tested at 40°C was moved to 20°C after 1000 cycles its capacity and ΔV matched those of the cell which had been cycled continuously at 20°C. Figures 12c and 12d show that when the cell tested at 55°C was moved to 20°C

after 1100 cycles its capacity and ΔV were close to those of the cell which had been cycled continuously at 20°C. The capacity of the cell after moving from 55 to 20°C (shown in Figure 12c) is lower than the cell which was tested entirely at 20°C because of lithium inventory loss during the 1100 cycles at 55°C. The results in Figure 12 demonstrate this cell chemistry is extremely tolerant to extended periods at elevated temperatures.

Long-term storage testing.—Figure 13 shows the results of long-term storage testing at 20, 40 and 55°C on the NMC532/graphite pouch cells containing electrolyte with 2%VC + 1% DTD additives. Figure 13 shows these cells behave in an outstanding manner during storage testing with little loss of capacity and minor increases in ΔV . Only the cell stored at 55°C and 4.3 V for 1.3 years shows signs of troublesome capacity loss and impedance growth. The combination of the additives 2% VC + 1% DTD with this single crystal NMC/artificial graphite chemistry is simply outstanding in storage.

Figure 14 shows the results of long-term storage testing at 20, 40 and 55°C on the NMC532/graphite pouch cells containing electrolyte with 1% LFO as the additive. Figure 14 shows that these cells have an inferior storage behavior at 40 and 55°C compared to the cells with the additive blend 2%VC + 1% DTD shown in Figure 13. It is believed that the reason for this inferior behavior is the lack of an effective negative electrode SEI former like VC or FEC. Unfortunately, given the excellent performance of cells with 2%FEC + 1% LFO in Figures 8, 10 and 11, storage data for cells with 2%FEC + 1%LFO is not mature enough to report at this time. The reason for showing the data in Figure 14 is to highlight that electrolyte additives make a huge difference to cell performance. The data presented in the reports on commercial cells^{2,3-8,10} used for lifetime modelling do not report the details of cell chemistry, including electrolyte additives, as we do here. We examine later below the reasons for the inferior performance of the cells with 1% LFO.

Figure 15 shows the drop in voltage of the cells during 3-month open circuit storage periods plotted as a function of the storage voltage for the cells in Figures 13 and 14. The average of the voltage drop during the last four 3-month storage periods (between 0.5 and 1.3 years in Figures 13 and 14) is shown. Figure 15 shows that the voltage drops during the storage periods are very small but that they increase with both storage voltage and temperature. Cells with 2% VC + 1% DTD show smaller voltage drops (less self-discharge) than cells with 1% LFO at both 40 and 55°C. The fitted lines to the data in Figure 15 are exponential in voltage. Figure 15b shows that the data appears to be exponentially activated in voltage based on the linearity of the data when plotted with a logarithmic y-axis.

Figure 16 shows the results of storage and charge-discharge cycling tests for NMC532/graphite cells with 2%VC + 1% DTD plotted on the same graph. This is a useful comparison to see the impact of exercising the cells on lifetime. The 55°C data show similar results for cells that were cycled or stored for the 1.3 years where the test results for both are available. This suggests that the major mechanism for capacity loss at 55°C is lithium inventory loss due to a thickening negative electrode SEI. At 20 and 40°C the cells undergoing charge-discharge testing lose slightly more capacity per unit time than the corresponding cells undergoing storage testing, however their rates of impedance growth, as monitored by $\Delta V/\Delta V_0$, are very similar. As will be shown later using differential voltage analysis (dV/dQ vs. Q) the major mechanism for capacity loss in cells tested at 40°C is lithium inventory loss due to a thickening negative electrode SEI. This accelerates during cycling due to the approx. 10% volume changes of the graphite particles during lithiation and delithiation.³ The cells at 20°C have lost only 4% capacity after 2.25 years and 3400 cycles. Differential voltage analysis does not have the resolution to determine the capacity loss mechanisms with such small capacity loss. However, by analogy to the 55°C and 40°C results it is believed the major loss mechanism is Li inventory loss at the negative electrode SEI for the cells that are cycling. This is consistent with the discussion of the C/20 capacity loss of the cells described by Figures 10 and 11.

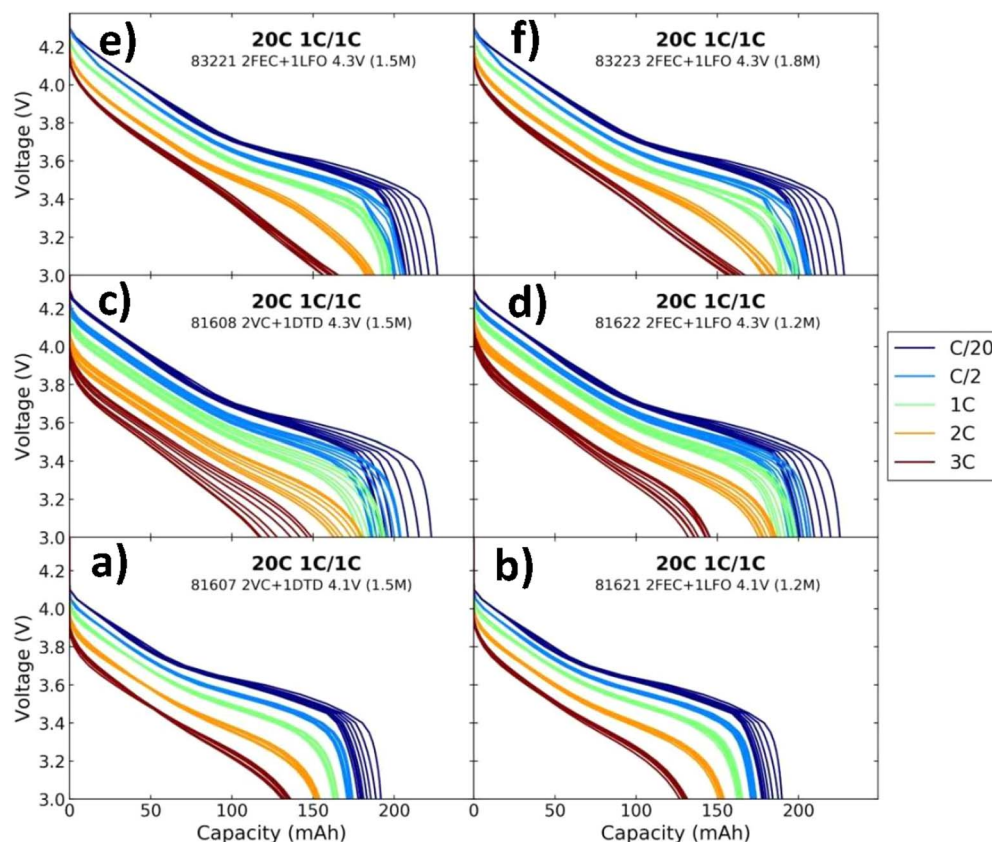


Figure 11. Voltage versus capacity for the C/20, C/2, 1C, 2C and 3C cycles of the discharge rate maps for the cells in Figure 10. The 8 curves of each color were taken at equally spaced intervals along the capacity versus cycle number curves. a) 1.5 M LiPF₆ in EC:EMC:DMC 25:5:70 with 2% VC + 1% DTD tested between 3.0 and 4.1 V; b) 1.2 M LiPF₆ in EC:EMC:DMC 25:5:70 with 2% FEC + 1% LFO tested between 3.0 and 4.1 V; c) 1.5 M LiPF₆ in EC:EMC:DMC 25:5:70 with 2% VC + 1% DTD tested between 3.0 and 4.3 V; d) 1.2 M LiPF₆ in EC:EMC:DMC 25:5:70 with 2% FEC + 1% LFO tested between 3.0 and 4.3 V; e) 1.5 M LiPF₆ in EC:EMC:DMC 25:5:70 with 2% FEC + 1% LFO tested between 3.0 and 4.3 V; f) 1.8 M LiPF₆ in EC:EMC:DMC 25:5:70 with 2% FEC + 1% LFO tested between 3.0 and 4.3 V.

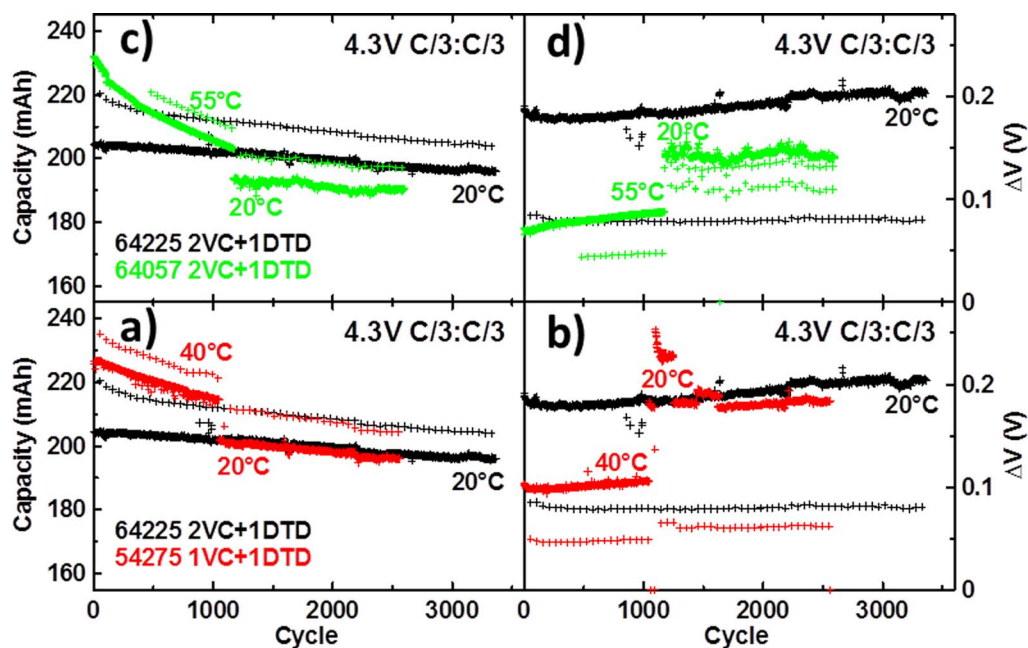


Figure 12. Capacity versus cycle number and ΔV versus cycle number for NMC532/graphite cells which were first cycled at elevated temperature, then moved to 20°C compared to cells which had been testing at 20°C continuously (black). a) Cell tested at 40°C then moved to 20°C (red) compared to a cell which had been at 20°C continuously; b) ΔV for the cells described by panel a); c) Cell tested at 55°C then moved to 20°C (green) compared to a cell which had been at 20°C continuously (black); d) ΔV for the cells described by panel c). All cells were tested at C/3 CCCV between 3.0 and 4.3 V. Electrolytes in these cells were 1.0 M LiPF₆ in EC:EMC 30:70 with additives listed in the figure legend.

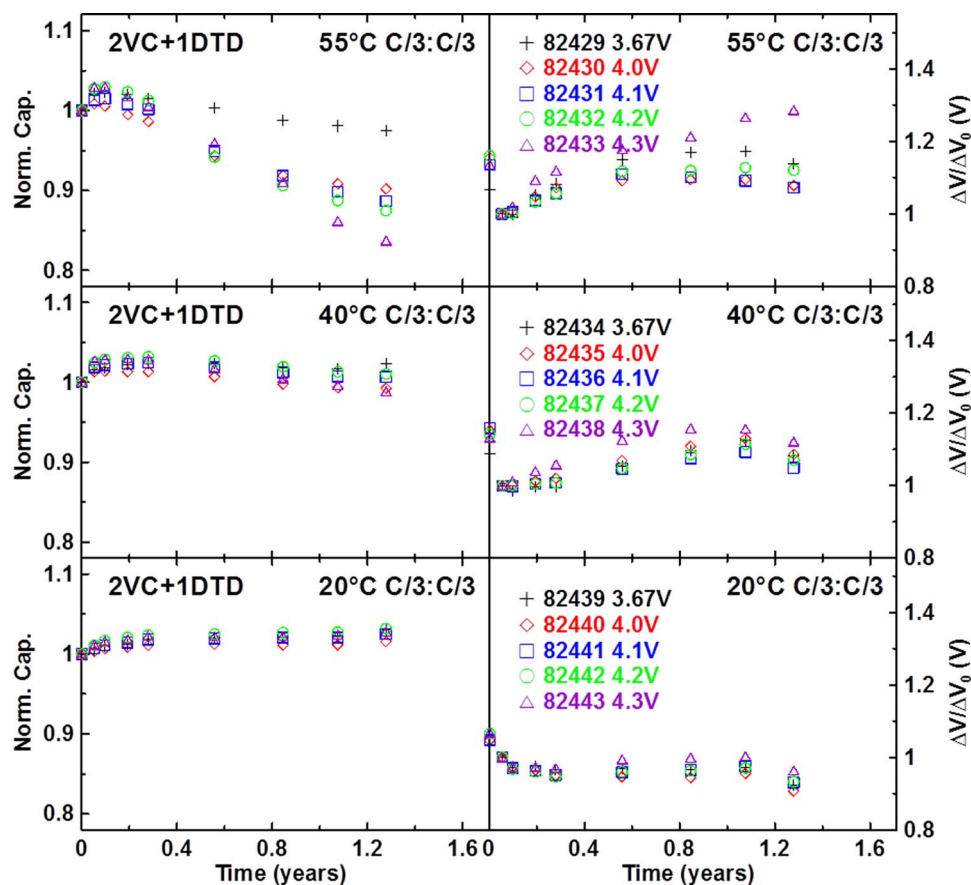


Figure 13. Long-term storage results for NMC532/graphite cells at 20, 40 and 55°C as indicated in the legend. Storage voltages were 3.67, 4.0, 4.1, 4.2 and 4.3 V. Normalized capacity and $\Delta V/\Delta V_0$ results were obtained from RPT performed at 20°C at the times indicated. These cells contained 2% VC + 1% DTD as the additive mixture.

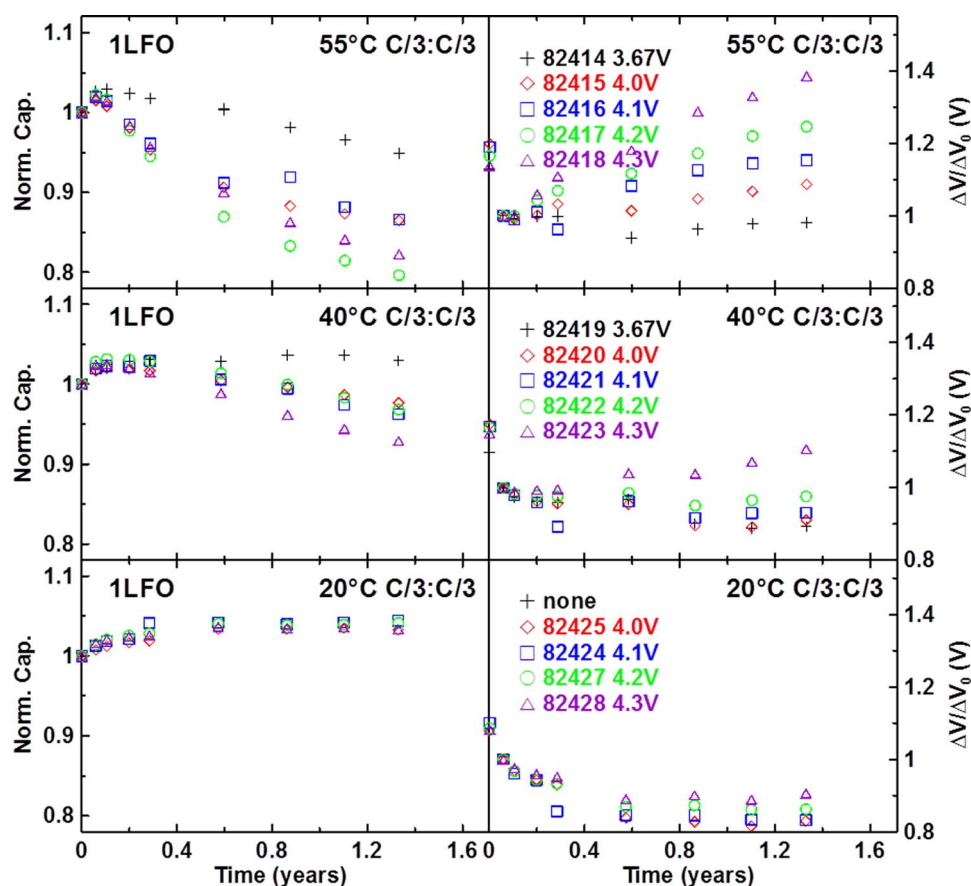


Figure 14. Long-term storage results for NMC532/graphite cells at 20, 40 and 55°C as indicated in the legend. Storage voltages were 3.67, 4.0, 4.1, 4.2 and 4.3 V. Normalized capacity and $\Delta V/\Delta V_0$ results were obtained from RPT performed at 20°C at the times indicated. These cells contained 1% LFO as the additive.

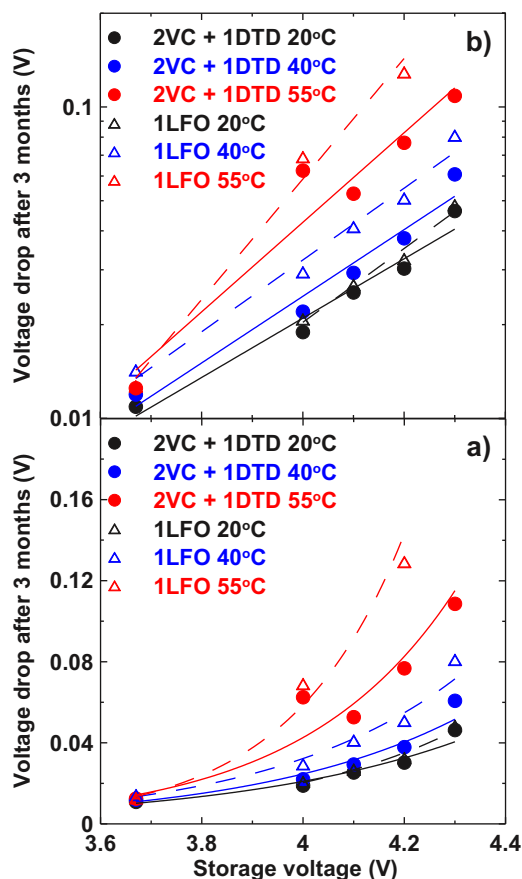


Figure 15. Voltage drop during the three month OCV storage periods for the cells in Figures 13 and 14 plotted versus storage voltage. The data plotted are the averages of the voltage drops during the last four 3-month storage periods in Figures 13 and 14. Electrolyte additives and storage temperatures are indicated in the legend.

Impact of methyl acetate on lifetime.—There is a large emphasis at the current time on lithium-ion cells with fast charge capability that do not sacrifice energy density. Modifications to the electrolyte that improve Li^+ diffusion can increase charging rates before the onset of lithium plating, however, there are lifetime penalties.^{21,22} Figure 17 shows the results of storage and charge-discharge cycling for NMC532/graphite cells with or without MA. At 20°C, there is little or no penalty in storage when MA is added, but capacity retention during cycling is compromised, especially for cells with 20% MA charged to 4.3 V, where rollover failure is observed after about one year of testing or 1700 C/3 cycles. Cells with MA cycled to 4.2 V show early indications of failure beginning after about 1.8 years or 2500 cycles. At 40°C, there are only comparative results available for cycle testing to 4.3 V. After two years of cycle testing, cells with 20% MA lost an additional 3% capacity compared to cells with no MA. Storage testing at 40°C shows that cells with MA lose capacity slightly faster, by about an extra 1% per year, compared to cells without MA.

The impact of MA on lifetime can be considered minor or major depending on the intended application of the cell. In a situation where high rate charge and discharge is required and intermittent use is envisaged (cells spend a large fraction of time in storage) the incorporation of MA would lead to a minor penalty at most. In addition, if the incorporation of MA eliminates Li plating during high rate charge, then MA would lead to a lifetime enhancement by removing this serious degradation pathway. On the other hand, if cells are intended to be cycled continuously between 3.0 and 4.3 V for years, Figure 17 suggests a major penalty associated with the incorporation of MA. Researchers contemplating the use of very thick electrodes even for low-rate Li-ion

cells will find the use of MA compelling. They should be aware that using MA will lead to lifetime penalties.

Ultra high precision charger testing.—The Ultra High Precision Charger (UHP) at Dalhousie University^{24,25} was used to measure the coulombic efficiency and charge endpoint capacity slippage of fresh and aged NMC532/graphite cells that contained 2% VC (or 1% VC) + 1% DTD or 2% FEC + 1% DTD additives. The UHP results were collected at 40°C between 3.0 and 4.3 V using currents corresponding to C/20. Figures 18a shows zeroed charge endpoint capacity, 18b shows discharge capacity, 18c shows coulombic efficiency (CE) and 18d shows ΔV , all plotted versus cycle number. Cells 54271 and 54275 were cycled 1000 times at 40°C between 3.0 and 4.3 V using currents corresponding to C/3 prior to being moved to UHP testing. Cell 54275 was previously highlighted in Figure 12a.

Figure 18a shows that the aged cells have virtually no charge endpoint capacity slippage. This means there are no species being oxidized at the positive electrode. Figure 18b shows that aged cells have virtually no capacity fade over 10 cycles in agreement with the long-term testing data. Figure 18c shows that the aged cells have coulombic efficiencies that very closely approach the perfect value of 1.00000.... Aged cell 54275 has an average CE between cycle 6 and 9 of 0.99985 ± 0.00003 suggesting the rate of parasitic reactions has become extremely small in this cell after aging. For comparison, UHP studies of aged LiCoO₂/graphite (LCO/graphite) cells have been reported by Fathi et al.²⁶ Cells that had been testing continuously for 11.7 years at C/6 charge and C/150 discharge between 3.0 and only 4.075 V at 37°C had accumulated 750 cycles and had 80% capacity remaining. These were then characterized by UHP. The CE of the aged LCO/graphite cells tested at 40°C between 3.0 and 4.075 V and with currents corresponding to C/20 was 0.99979 ± 0.00002 .²⁶ The fact that the aged NMC532/graphite cells tested between 3.0 and 4.3 V had a CE higher than those of the aged LCO/graphite cells suggests the lifetime of the NMC532/graphite cells will be extremely long.

Degradation mechanisms of the NMC532/graphite cells.—Differential voltage analysis (dV/dQ vs. Q) has been shown by Bloom et al. and Honkura et al.^{27–29} to be very effective in elucidating degradation mechanisms in Li-ion cells. Our laboratory has implemented dV/dQ analysis in a user-friendly software package³⁰ which was utilized here. Five NMC532/graphite cells with 2% VC + 1% DTD additives were cycled 0, 200, 400, 700 and 900 cycles between 3.0 and 4.3 V at 40°C at C/3. After those cycles, cells were moved to the UHP where high fidelity measurements of dV/dQ vs. Q and dQ/dV vs. V were collected. Positive and negative electrode reference curves required for dV/dQ analysis were collected in half coin cells using electrodes extracted from new, dry (no electrolyte) pouch cells.

Figure 19 shows the results of dV/dQ analysis on these cells. Figure 19a shows the full cell voltage curves and the voltage versus capacity curves of the positive and negative electrodes versus lithium. The charge axis in Figure 19a is zero at the point where the full cell is fully discharged. Figures 19b and 19c show the excellent agreement between the calculated and measured values of dV/dQ vs. Q and dQ/dV vs. V , respectively. Figures 19d and 19e show the cells capacity and $\Delta V/\Delta V_0$, respectively, versus cycle number. Figures 19f, 19g and 19h show the relative electrode shift or slippage (due lithium inventory loss), the positive electrode capacity and the negative electrode capacity, respectively, for the five cells plotted versus cycle number. Figure 19d shows that over the 900 cycles the cells lost about 11 mAh of capacity. Figure 19e shows that over the same period the shift loss, due to Li inventory loss was about 9 mAh, in good agreement. Figures 19f and 19g show no evidence for loss of positive or negative electrode capacity. Based on these experiments one concludes that Li inventory loss, due to thickening of the negative electrode SEI, is the major degradation mechanism for these cells. Figure 19e also shows that there is a small impedance growth in the cells.

Practitioners of dV/dQ analysis will appreciate that it is hard to be absolutely certain of dV/dQ analysis results when a cell has only lost a few percent of capacity as in Figure 19. Therefore, dV/dQ analysis was

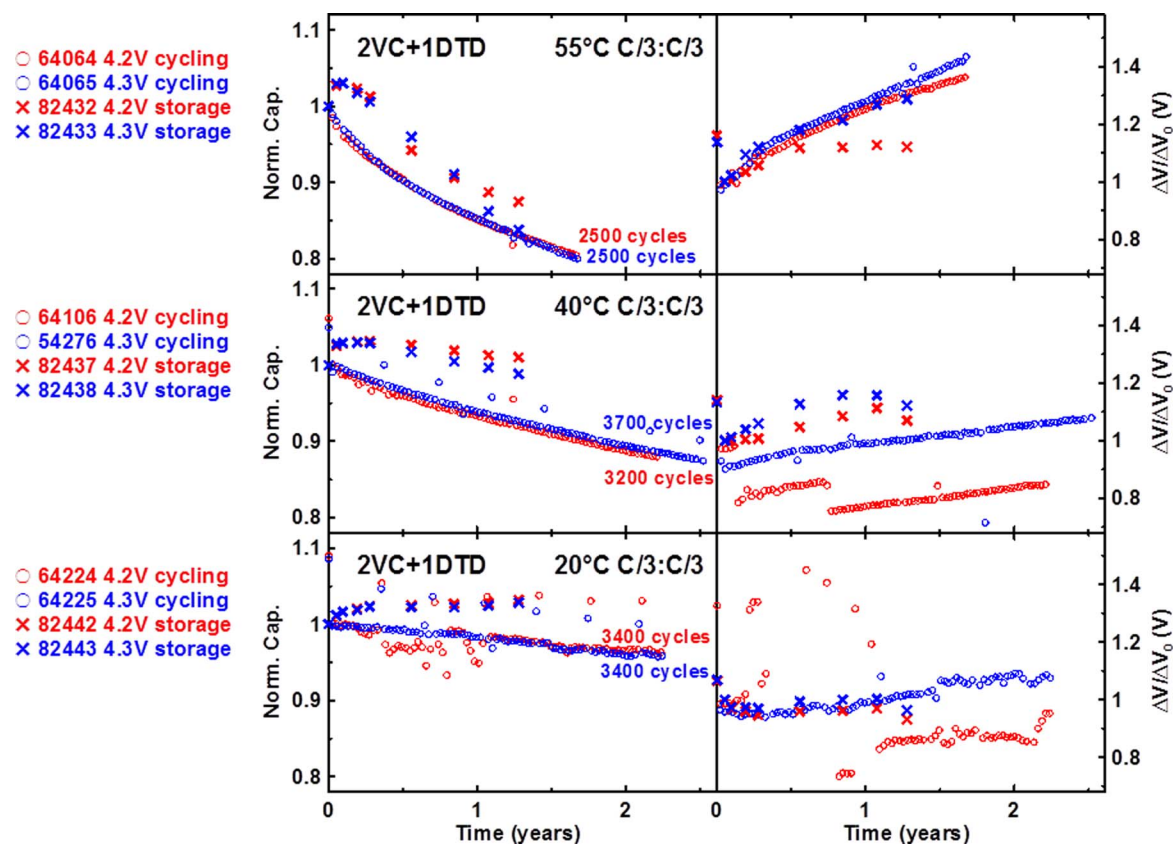


Figure 16. Normalized capacity and $\Delta V/\Delta V_0$ plotted versus time for NMC532/graphite cells undergoing cycling or storage testing at 20, 40 and 55°C. The charge-discharge cycling was performed at C/3 between 3.0 and 4.3 V (blue circles) or between 3.0 and 4.2 V (red circles). The storage testing was done at 4.3 V (blue crosses) or at 4.2 V (red crosses). Normalized capacity for the storage testing was measured with the RPT protocol (Figure 7) at 20°C. The cells contained 2% VC + 1% DTD as additives.

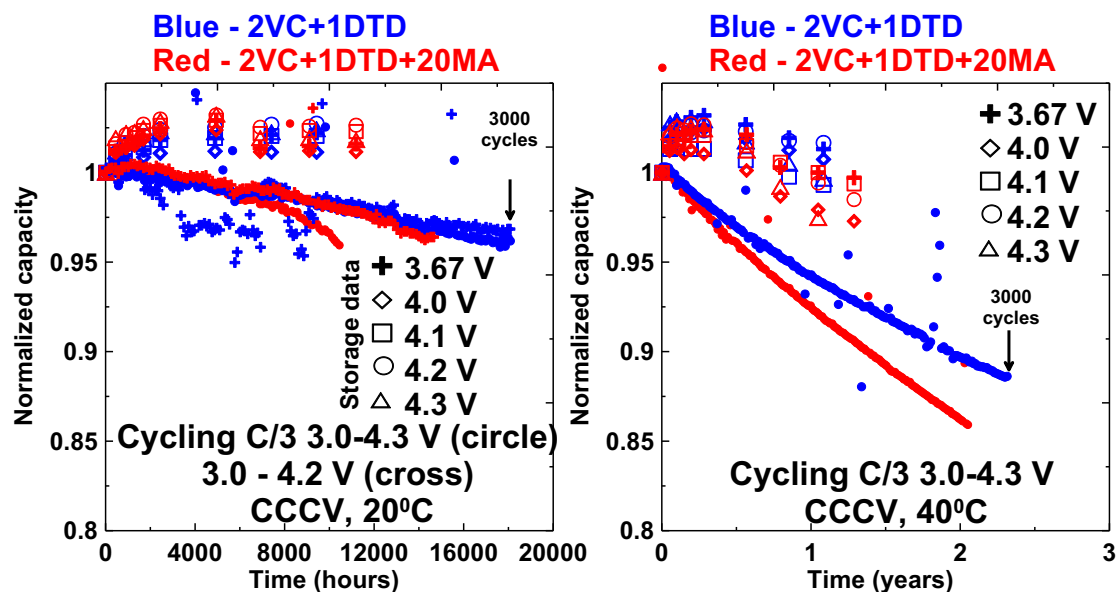


Figure 17. Normalized capacity plotted versus time for NMC532/graphite cells undergoing cycling or storage testing at 20 and 40°C. The charge-discharge cycling was performed at C/3 between 3.0 and 4.3 V (circles) or between 3.0 and 4.2 V (crosses). The storage testing was done at the voltages indicated in the legend. Results for cells that had 20% MA in the electrolyte are shown in red and results for cells that had no MA are shown in blue. Normalized capacity for the storage testing was measured with the RPT protocol (Figure 7) at 20°C. The cells contained 2% VC + 1% DTD as additives.

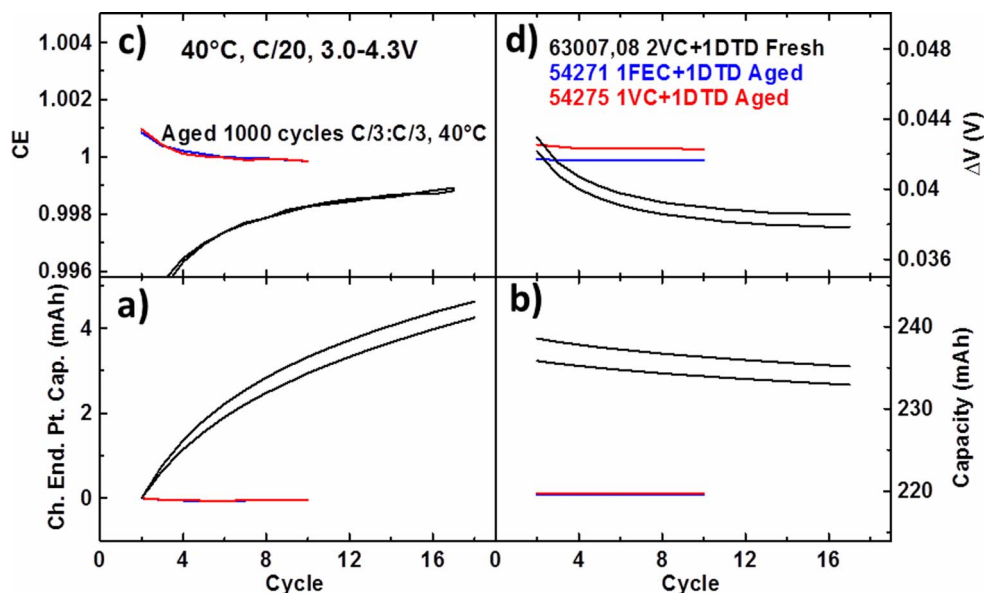


Figure 18. Ultra high precision charger (UHP) results for fresh and aged NMC532/graphite cells containing the electrolyte additives listed in the legend. The UHP results were collected at 40°C between 3.0 and 4.3 V using currents corresponding to C/20. a) zeroed charge endpoint capacity; b) discharge capacity; c) coulombic efficiency (CE); and d) ΔV . Cells 54271 and 54275 were cycled 1000 times at 40°C between 3.0 and 4.3 V using currents corresponding to C/3 prior to being moved to UHP testing. Cell 54275 was previously highlighted in Figure 12a.

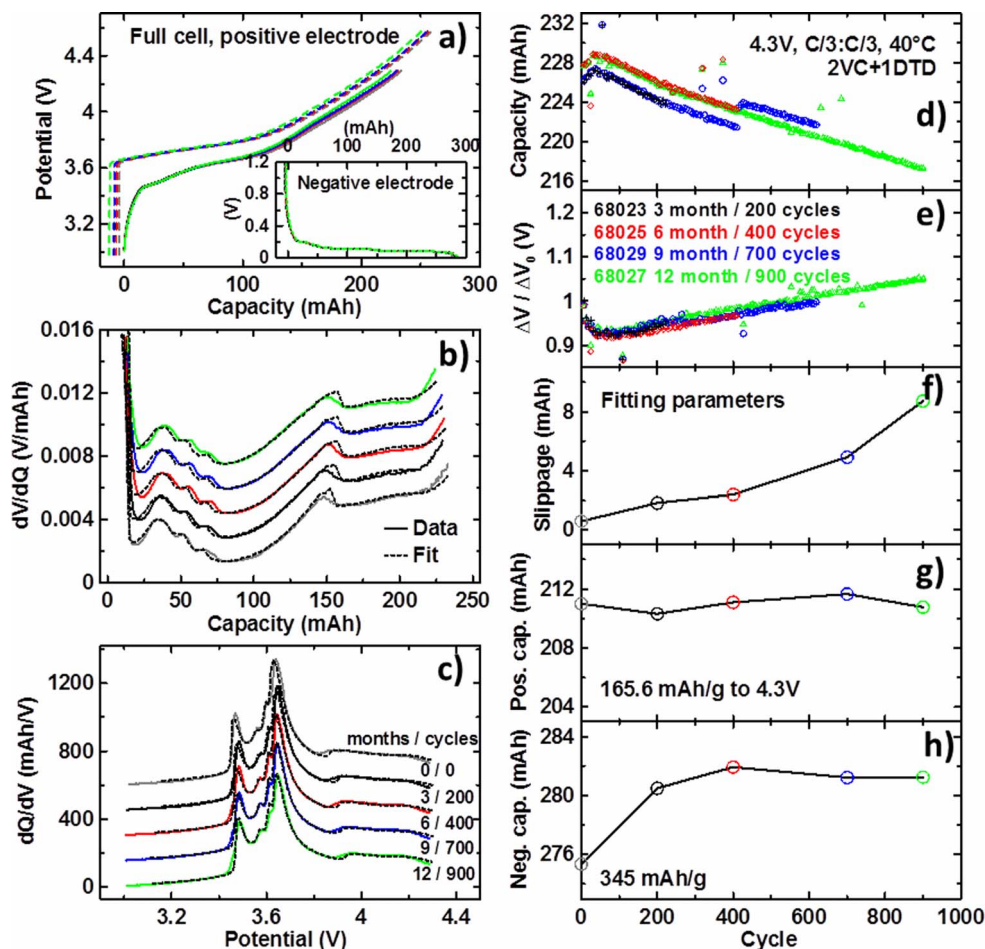


Figure 19. Differential voltage analysis of NMC532/graphite cells tested at C/3 and 40°C between 3.0 and 4.3 V. a) the full cell voltage curves and the voltage versus capacity curves of the positive and negative electrodes versus lithium for five cells cycled 0, 200, 400, 700 and 900 times. The charge axis in Figure 18a is zero at the point where the full cell is fully discharged; b) the calculated and measured values of dV/dQ vs. Q ; c) the calculated and measured values of dQ/dV vs. V ; d) the cell capacity versus cycle number; e) $\Delta V/\Delta V_0$ versus cycle number; f) the relative electrode shift or slippage (due to lithium inventory loss) versus cycle number; g) the positive electrode capacity vs. cycle number; h) the negative electrode capacity versus cycle number.

performed on a more heavily cycled NMC532/graphite cell containing 2% VC + 1% DTD which was tested at 55°C (C/3 between 3.0 and 4.3 V) for 20 months. High fidelity data for dQ/dV vs V and dV/dQ vs Q was available after 0, 100 and 2500 cycles. This cell was from a different build compared to the cell considered in Figure 19. It had more excess negative electrode so it could be charged to 4.5 V without Li plating, if desired. Figure 20 shows the results of dV/dQ analysis on the cell cycled at 55°C. Figure 20 has the same format as Figure 19. Figure 20d shows that over the 2500 cycles the cell lost about 45 mAh of capacity. Figure 20e shows that over the same period the shift loss, due to Li inventory loss, was about 42 mAh, in good agreement. Figures 20f and 20g show evidence for a small loss of positive (6 mAh) and negative electrode (4 mAh) capacity, both about an order of magnitude smaller than the shift loss and hence very small. Just as the experiment considered in Figure 19, one concludes that Li inventory loss, due to thickening of the negative electrode SEI, is the major degradation mechanism for this cell. Figure 20e also shows that there is a significant impedance growth in this cell presumably due to the high temperature of operation and the 20 month duration of the test.

The volumes of gas generated in many of the cells under long-term testing were measured using Archimedes principle as described in the experimental section of reference.²² The experiments on the cylindrical cells reported in the literature^{2,5-9} give no indication of gas generated during cycling or storage. Figure 21 shows the volume of

gas generated in NMC532/graphite cells during long-term cycling and storage at 20, 40 and 55°C for cells with 2%VC + 1%DTD and cells with 1% LFO as additives. As shown in Table I, the volumes of the cells themselves are 2.3 mL. Figure 21 shows that gassing is not an issue for cells cycled or stored at 20°C. Figure 21 shows that cells with 2%VC + 1%DTD undergoing continuous cycling at 40°C generate minimal gas even after 2.5 years of 100% DOD cycling. Figure 21 shows that cells with 1%LFO generate more gas than cells with 2%VC + 1%DTD under all conditions and untenable amounts of gas at 55°C. Unfortunately, comprehensive data for cells with the additive system 2%FEC + 1% LFO are not available yet. Gas generation in the cells with 2%VC + 1%DTD cycled or stored continuously at 55°C may also be problematic. It is not known what volume of gas produced in these small pouch cells would correspond to the amount needed to open the pressure activated vent in a cylindrical or prismatic cell.

The increased gassing in cells with 1% LFO stored at 40 and 55°C compared to cells with 2% VC + 1% DTD correlates well with the differences in their storage performance shown in Figures 13 and 14. Gas generation is caused by reactions between the charged electrode materials and the electrolyte. Therefore one can roughly say that when there is little gassing there are few parasitic reactions occurring in the cells. The gas volume data at 20°C suggests very few parasitic reactions and correlates well with the excellent long-term cycling of these cells at 20°C (Figures 8, 9 and 10) with little impedance growth.

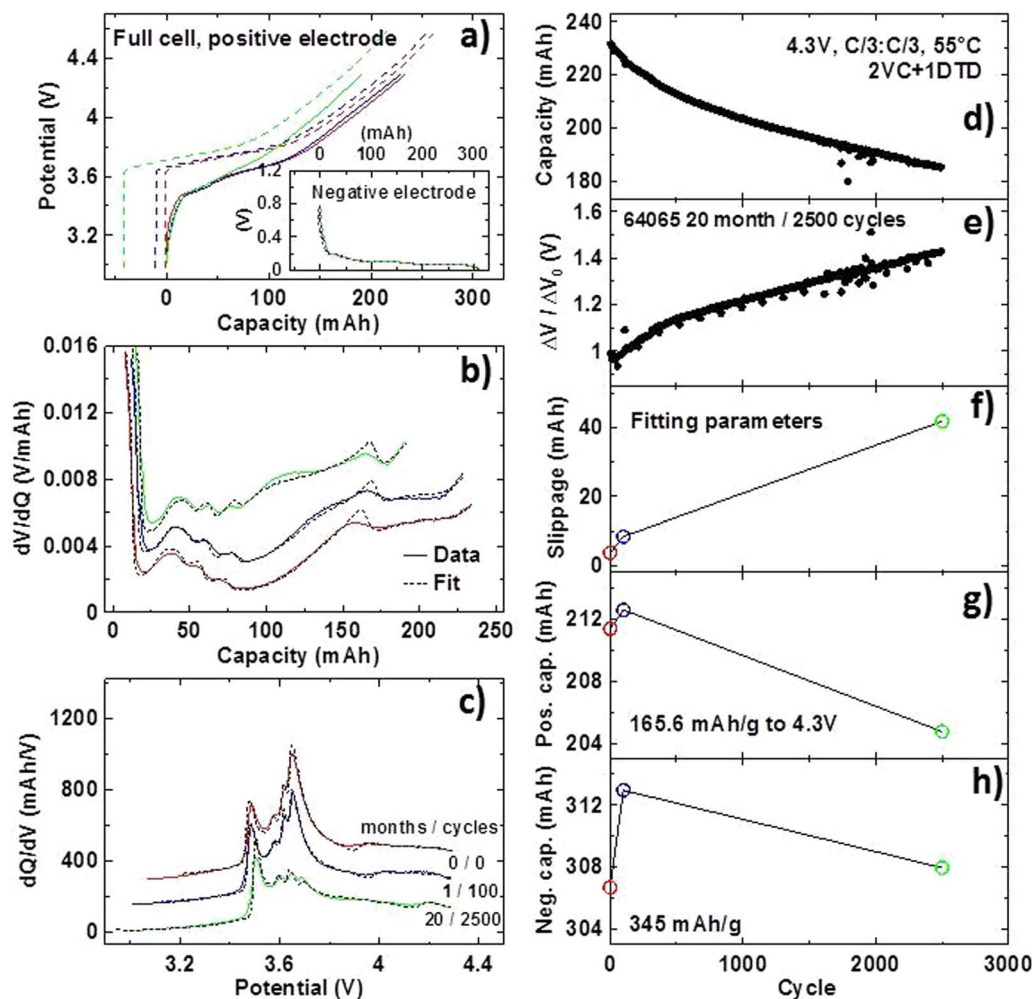


Figure 20. Differential voltage analysis of a NMC532/graphite cell tested at C/3 and 55°C between 3.0 and 4.3 V. a) the full cell voltage curves and the voltage versus capacity curves of the positive and negative electrodes versus lithium for the same cell at cycle 0, 100, and 2500. The charge axis in Figure 18a is zero at the point where the full cell is fully discharged; b) the calculated and measured values of dV/dQ vs. Q ; c) the calculated and measured values of dQ/dV vs. V ; d) the cell capacity versus cycle number; e) $\Delta V/\Delta V_0$ versus cycle number; f) the relative electrode shift or slippage (due to lithium inventory loss) versus cycle number; g) the positive electrode capacity vs. cycle number; h) the negative electrode capacity versus cycle number.

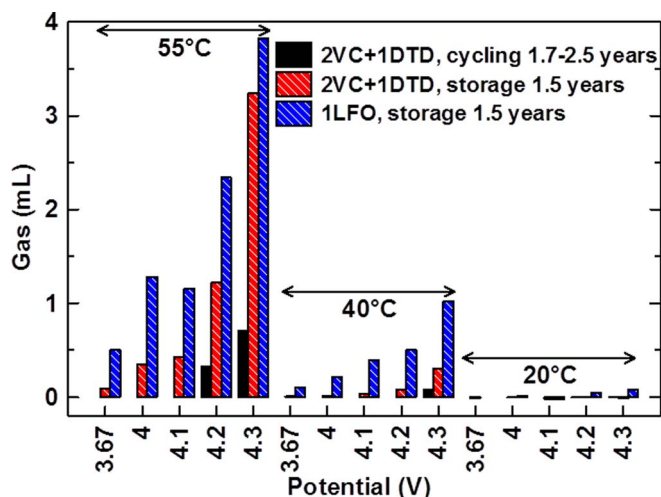


Figure 21. Volume of gas generated during cycling and storage in the NMC532/graphite cells with electrolyte additives listed in the legend. The storage potential or the upper cutoff potential during cycling is indicated along the x-axis for the three temperatures considered: 55, 40 and 20°C. The gas bags in these cells can hold about 2.5 ml of gas before the gas begins to be compressed above atmospheric pressure. This means gas volumes measured by Archimedes principle that are greater than 2.5 mL would be even greater if the gas were at 1 atm pressure.

The small gas volumes generated at 20°C also correlate well with the excellent storage behavior of these cells at 20°C with virtually no capacity loss nor impedance growth (Figures 13 and 14).

Virtually no micro-cracking in the single crystal NMC532 electrode particles after 5000 cycles.—A cell (barcode 82306) containing

the electrolyte additives 2% VC + 1% DTD was tested for 5300 cycles at 20°C using currents corresponding to 1C. The voltage limits were 3.0 to 4.1 V. The cell had 97% of its initial capacity remaining much like the results for the cell shown in Figure 10a which was tested under the same conditions. After 5300 cycles the cell was charged to 4.3 V at C/20 and then opened in a glove box. The positive electrode was cross-sectioned and imaged as described in the experimental section.

Figure 22 shows representative cross sectional SEM images of the electrode particles after 5300 cycles. No evidence of micro-cracking can be observed in particles that were initially less than 3 micrometers in size, demonstrating again the advantages of single crystal materials. This why there is no loss of positive electrode active mass in these cells during cycling. Figure 22 suggests that the cell in Figure 10a would have an incredibly long cycle life. The paper by Li et al.³¹ introduces the advantages of single crystal materials compared to conventional polycrystalline positive electrode materials.

What might be the lifetime of these NMC532/graphite cells?—It is interesting to consider the possible lifetime of these cells in EV and grid storage applications. Complex models are not used here. Consider the data in Figures 10, 11 and 16. At 20°C cells can be cycled at either 1C or C/3 for 4000 100% DOD cycles with about 4% capacity loss and less than 10% impedance growth. The fractional capacity loss rate is therefore about 0.00001/cycle. At 20°C cells can be stored at full charge for 1.3 years with about 0% loss and no impedance change and at 90% charge with 0% loss and no impedance change. The capacity loss rate is 0.0/year. At 40°C, cells can be cycled at C/3 for 3700 100% DOD cycles with about 12% capacity loss and about 15% impedance growth. The fractional capacity loss rate at 40°C is about 0.000032/cycle. At 40°C, cells can be stored at full charge for 1.3 years with about 3% loss and 10% impedance change or at 90% charge with about 1.5% loss and 8% impedance change. The fractional capacity loss rate during 100% DOD storage at 40°C is about 0.02/year.

Assume a use scenario that blends storage (worst case scenario at top of charge) and cycling (worst case scenario 100% DOD) and

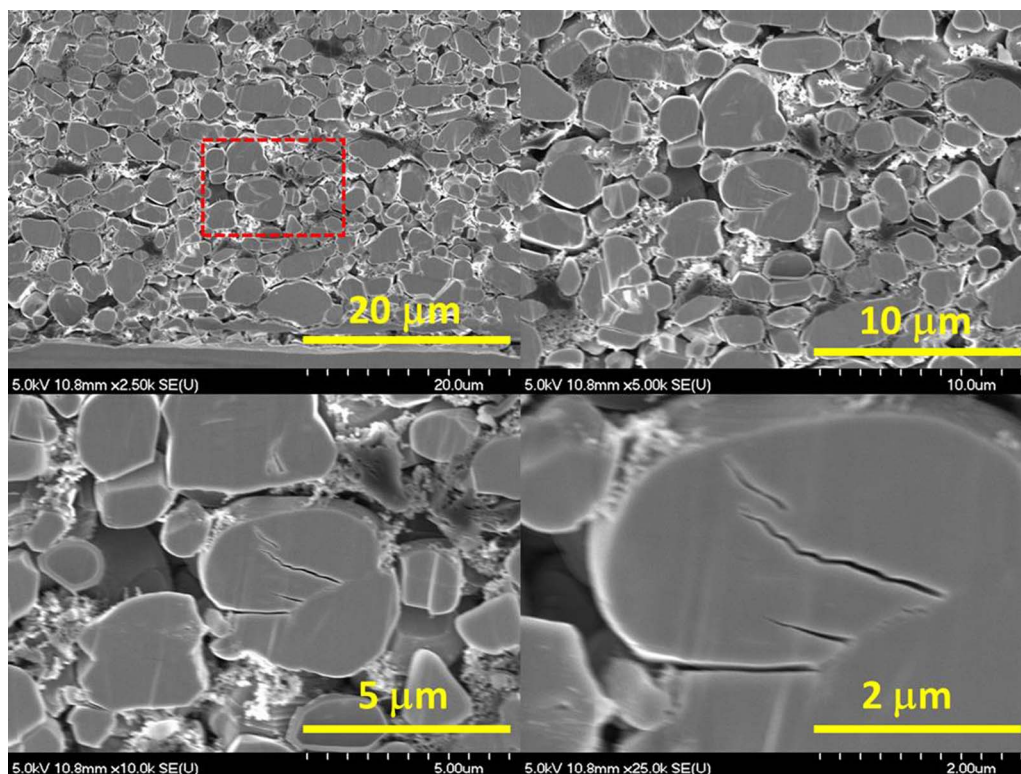


Figure 22. Cross sectional SEM of a single crystal NMC532 positive electrode taken from a cell tested exactly under the conditions of the cell in Figure 10a. The cell had 97% capacity retention after 5300 cycles. Notice that there are virtually no microcracks in any of the electrode particles. This is why these cells show no loss of positive electrode active mass during cycling.

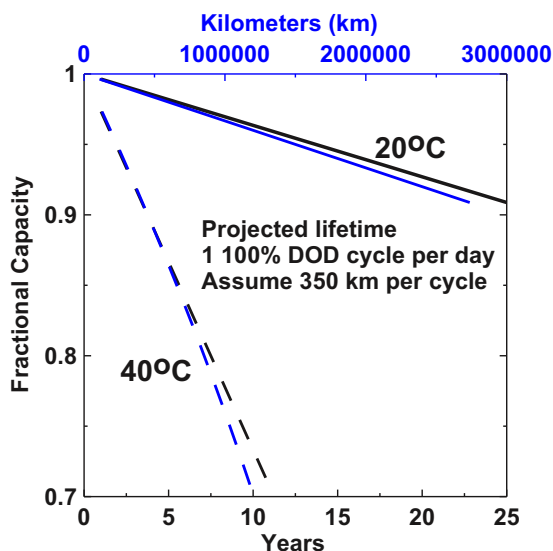


Figure 23. Worst-case scenario lifetime and total driving range projections for the NMC532/graphite cells with 2% VC + 1% DTD at 20 and 40°C. Assumptions made were one 6 hour 100% DOD cycle per day and 350 km initial driving range per cycle. Equation 1, with $M = 1$, $n = 3$, $L_c = 0.00001/\text{cycle}$ (20°C), $L_c = 0.000032/\text{cycle}$ (40°C), $L_s = 0.0/\text{year}$ (20°C) and $L_s = 0.02/\text{yr}$ (40°C) was used to calculate Q/Q_0 .

cycling in a mode where there are M 100% DOD cycles per day at an average C/n rate. That means the time of cycling each day would be $2 M n$ hours. The time of storage would be $24 - 2 M n$. The fractional capacity as a function of time in years would be:

$$Q/Q_0 = 1 - L_c M 365 t - L_s (24 - 2 M n) / 24 t \quad [1]$$

where L_c is the fractional loss per cycle, L_s is the fractional loss per year during storage and t is the time in years. This assumes that all degradation processes are linear and do not slow with time. Again, this is a worst case scenario.

Figure 23 shows the projected fractional capacity of these NMC532/graphite cells as a function of time in years in a scenario where the cells are cycled once per day (100% DOD to 4.3 V) in a cycling event that takes 6 hours. It is also assumed that during the remaining time, cells are stored at full state of charge. It is clear from Figure 23 that these cells would provide an exceptionally long total driving range in an EV if the cells were maintained at an average temperature of 20°C. Even if the cells were continually at 40°C, 10 years of lifetime to 70% capacity and a total driven distance of 1,200,000 km is projected. It is worth noting that only 3650 cycles would be required for this total driven distance and 3700 cycles have been demonstrated in Figure 16.

Most important to realize is that Figure 23 assumes 100% DOD cycling on every cycle and storage at full state of charge. If the reader reviews the literature data in Figures 1 and 2, the reader will realize that the lifetime will be much better in situations where the DOD is limited and in situations where cells are stored at lower states of charge. Admittedly, the projections in Figure 23 use the incredibly simple model described by equation 1. It is our opinion that more sophisticated models will lead to even longer lifetime projections.

Conclusions

Single crystal NMC532/graphite cells with exceptional lifetime have been developed. Storage and cycle testing up to 3 years in duration has been presented at 20, 40 and 55°C. The lifetime of these cells far exceeds that of other NMC/graphite cells reported in the literature and which have been used for lifetime modelling. It is suggested

that lifetime models for NMC532/graphite cells consider the data presented here.

Full details of these cells including electrode compositions, electrode loadings, electrolyte compositions, additives used, etc. have been provided in contrast to literature reports using commercial cells. This has been done so that others can re-create these cells and use them as benchmarks for their own R+D efforts be they in the spaces of Li-ion cells or “beyond Li-ion cells”.

The cells described here have two dominant failure mechanisms at 20, 40 and 55°C. These are Li inventory loss and impedance growth. We find virtually no evidence for loss of active material in these cells during cycle testing under the conditions used here.

The numeric data used in Figures with cell barcode labels indicated can be made available to interested readers. Please contact the authors.

Acknowledgments

The work done here was supported by NSERC and Tesla Canada under the auspices of the Industrial Chairs program. Many of the authors have received scholarship support from NSERC, the China Scholarship Council and the Nova Scotia Graduate Scholarship program and that support is gratefully acknowledged.

ORCID

Jessie E. Harlow <https://orcid.org/0000-0002-3928-2573>
 Stephen L. Glazier <https://orcid.org/0000-0003-2961-3049>
 J. R. Dahn <https://orcid.org/0000-0002-6997-2436>

References

1. N. S. Pearre, W. Kempton, R. L. Guensler, and V. V. Elango, *Transp. Res. Part C Emerg. Technol.*, **19**, 1171 (2011).
2. M. Ecker et al., *J. Power Sources*, **248**, 839 (2014).
3. R. D. Deshpande and D. M. Bernardi, *J. Electrochem. Soc.*, **164**, A461 (2017).
4. Z. Gao et al., *Energy*, **122**, 588 (2017).
5. A. Jana, G. M. Shaver, and R. E. García, *J. Power Sources*, **422**, 185 (2019).
6. J. Schmitt, A. Maheshwari, M. Heck, S. Lux, and M. Vetter, *J. Power Sources*, **353**, 183 (2017).
7. S. F. Schuster et al., *J. Energy Storage*, **1**, 44 (2015).
8. M. Dubarry, N. Qin, and P. Brooker, *Curr. Opin. Electrochem.*, **9**, 106 (2018).
9. P. Keil et al., *J. Electrochem. Soc.*, **163**, A1872 (2016).
10. M. Naumann, M. Schimpe, P. Keil, H. C. Hesse, and A. Jossen, *J. Energy Storage*, **17**, 153 (2018).
11. P. Keil and A. Jossen, *J. Electrochem. Soc.*, **164**, A6066 (2017).
12. J. Li, H. Li, W. Stone, S. Glazier, and J. R. Dahn, *J. Electrochem. Soc.*, **165**, A626 (2018).
13. L. Ma et al., *J. Electrochem. Soc.*, **165**, A891 (2018).
14. L. Ma et al., *ACS Appl. Energy Mater.*, **1**, 7052 (2018).
15. L. Ma, L. Ellis, S. L. Glazier, X. Ma, and J. R. Dahn, *J. Electrochem. Soc.*, **165**, A1718 (2018).
16. X. Ma et al., *J. Electrochem. Soc.*, **166**, A711 (2019).
17. D. Y. Wang et al., *J. Electrochem. Soc.*, **161**, A1818 (2014).
18. D. Y. Wang, N. N. Sinha, R. Petibon, J. C. Burns, and J. R. Dahn, *J. Power Sources*, **251**, 311 (2014).
19. L. Ma et al., *J. Electrochem. Soc.*, **161**, A1261 (2014).
20. J. R. Dahn, G. Erlich, and D. Doughty, *Linden's Handbook of Batteries*, Chapter 17 K. Beard, Editor, 5th ed., p. 755, McGraw-Hill, (2019).
21. E. R. Logan et al., *J. Electrochem. Soc.*, **165**, A21 (2018).
22. J. Li et al., *J. Electrochem. Soc.*, **165**, A1027 (2018).
23. K. L. Gering, *Electrochim. Acta*, **225**, 175 (2017).
24. T. M. Bond, J. C. Burns, D. A. Stevens, H. M. Dahn, and J. R. Dahn, *J. Electrochem. Soc.*, **160**, A521 (2013).
25. A. J. Smith, J. C. Burns, S. Trussler, and J. R. Dahn, *J. Electrochem. Soc.*, **157**, A196 (2009).
26. R. Fathi et al., *J. Electrochem. Soc.*, **161**, A1572 (2014).
27. I. Bloom, J. P. Christophersen, D. P. Abraham, and K. L. Gering, *J. Power Sources*, **157**, 537 (2006).
28. I. Bloom et al., *J. Power Sources*, **139**, 295 (2005).
29. K. Honkura, H. Honbo, Y. Koishikawa, and T. Horiba, *ECS Transactions*, **13**, 61 (2008).
30. H. M. Dahn, A. J. Smith, J. C. Burns, D. A. Stevens, and J. R. Dahn, *J. Electrochem. Soc.*, **159**, A1405 (2012).
31. J. Li et al., *J. Electrochem. Soc.*, **164**, 1534 (2017).